Frequency upon Image Enhancement by using Transform

Dr. N. Geetha Rani[1], Y. Chandu Priya[2], T. Moksha Sai Devi[3], S. Aneesa Fathima[4], S. Mounika[5]

[1]Associate Professor, Department of ECE, Ravindra college of Engineering for Women, Kurnool, Andhra Pradesh, India

[2,3,4 & 5]Department of ECE, Ravindra college of Engineering for Women, Kurnool, Andhra Pradesh, India

ABSTRACT

The purpose of multi-focus image fusion is to gather the essential information and the focused parts from the input multi-focus images into a single image. These multi-focus images are captured with different depths of focus of cameras. A lot of multi-focus image fusion techniques have been introduced using the focus measurement in the spatial domain. However, multi-focus image fusion processing is very time-saving and appropriate in discrete cosine transform (DCT) domain, especially when JPEG images are used in visual sensor networks. Thus most of the researchers are interested in focus measurement calculations and fusion processes directly in the DCT domain. Accordingly, many researchers have developed some techniques that substitute the spatial domain fusion process with the DCT domain fusion process. Previous works on the DCT domain have some shortcomings in the selection of suitable divided blocks according to their criterion for focus measurement. In this paper, calculation of two powerful focus measurements, proposed directly in the DCT domain. Moreover, two other new focus measurements that work by measuring the correlation coefficient between the source blocks, and the artificial blurred blocks are developed completely in the DCT domain. However, a new consistency verification method is introduced as a post-processing, significantly improving the quality of the fused image. These proposed methods significantly reduce the drawbacks due to unsuitable block selection. The output image quality of our proposed methods is demonstrated by comparing the results of the proposed algorithms with the previous ones.

Keywords : Image Fusion, Multi-Focus, Visual Sensor Networks, Discrete Wavelet Transform, Discrete Cosine Transform.

I. INTRODUCTION

The image fusion process is defined as gathering all the important information from multiple images, and their inclusion into fewer images, usually a single one. This single image is more informative and accurate than any single source image, and it consists of all the necessary information. The purpose of image fusion is not only to reduce the amount of data but also to construct images that are more appropriate and understandable for the human and machine perception [1]. The ideal image consists of all the scene components that are

completely transparent but due to intrinsic limitations in the system, it may not have a single image of the scene including all the necessary information and description of the object details. The main reason is the limited depth of focus in the optical lenses of CCD/CMOS cameras [2, 3]. Therefore, those objects that are only located in the special depth of focus are clear, and the others are blurred. To solve this problem, it is recommended to record multiple images of a scene with different depths of focus. The main idea of this work is to focus all the components in multiple captured images. Fortunately, in visual sensor networks (VSNs), there is a capability to increase the different depths of focus using a large number of cameras [4, 5]. In VSN, sensors are cameras recording images and video sequences. Despite its advantages, it has some limitations such as energy consumption, power, processing time, and limited bandwidth. Due to a huge amount of data created by camera sensors compared with the other sensors e.g. pressure, temperature, and microphone, energy consumption plays an important role in the lifetime of camera sensors [6, 7]. Therefore, it is important to process the local input images. In VSN, there are many camera nodes that are able to process the captured images locally, and collect the necessary information [8]. Due to the aforementioned reasons, multi-focus image fusion is manifested. It is a process that produces an image with all the unified components of a scene by merging multiple images with different depths of focus on the scene.

II. RELATED WORKS

Several works have been carried out on image fusion in the spatial domain . Many of these methods are complicated and suffer from being time-consuming as they are based upon the spatial domain. Image fusion based on the multi-scale transform is the most commonly used and very promising technique. Laplacian pyramid transform , gradient pyramid-based transform , morphological pyramid transform and the premier ones, discrete wavelet transform (DWT) , shift-invariant wavelet transform (SIDWT) , and discrete cosine harmonic wavelet transform (DCHWT) are some examples of the image fusion methods based on the multi-scale transform. These methods are complex and have some limitations e.g. processing time and energy consumption. For example, the multi-focus image fusion methods based on DWT require a lot of convolution operations, so it takes more time and energy for processing. Therefore, most of methods used in the multi-scale transform are not suitable for performing in real-time applications . Moreover, these methods are not very successful in edge places due to missing the edges of the image in the wavelet transform process. However, they create ringing artefacts in the output image and reduce its quality.

Due to the aforementioned problems in the multi-scale transform methods, researchers are interested in multi-focus image fusion in the discrete cosine transform (DCT) domain. The DCT-based methods are more efficient in terms of

transmission and archiving images coded in Joint Photographic Experts Group (JPEG) standard to the upper node in the VSN agent. A JPEG system consists of a pair of encoder and decoder. In the encoder, images are divided into non-overlapping 8×8 blocks, and the DCT coefficients are calculated for each one of them. Since the quantization of DCT coefficients is a lossy process, many of the small-valued DCT coefficients are quantized to zero, which correspond to high frequencies. The DCT-based image fusion algorithms work more properly when the multi-focus image fusion methods are applied in the compressed domain . In addition, in the spatial-based methods, the input images must be decoded and then transferred to the spatial domain. After implementation of the image fusion operations, the output fused images must again be encoded . Therefore, the DCT domain-based methods do not require complex and time-consuming consecutive decoding and encoding operations.

Therefore, the image fusion methods based on DCT domain operate with an extremely less energy and processing time.

Recently, a lot of research works have been carried out in the DCT domain. Tang has introduced the DCT+Average and DCT+Contrast methods for multi-focus image fusion in the DCT domain. In the DCT+Average method, a fused image is created by a simple average of all DCT coefficients of input images. To create the DCT coefficients of the output 8×8 block in the DCT+Contrast method, the maximum coefficient value is selected for all 63 AC coefficients of input blocks, and the average DC coefficients for all the input image block is selected for DC coefficient of the output block. These two methods suffer from undesirable side-effects like blurring and blocking effects, so the output image quality is reduced.

Most of the DCT domain methods are inspirited from the spatial domain methods. Since the implementation of all focus measurements in the spatial domain is very easy and simple, researchers try to implement the algorithms in the DCT domain after a satisfactory calculation of the focus measurements in the spatial domain. Huang and Jing have reviewed and applied several focus measurements in the spatial domain for the multi- focus image fusion process, which are suitable for real-time applications [9]. They mentioned some focus measurements including variance, energy of image gradient (EOG), Tenenbaum''s algorithm (Tenengrad), energy of Laplacian of the image (EOL), sum-modified-Laplacian (SML), the DCT domain. Thus this paper introduces the EOL and VOL calculations completely in the DCT domain.

Finally, CV as a post-processing in multi- focus image fusion algorithms is enhanced by introducing repeated consistency verification (RCV). This process greatly enhances the decision map for constructing the output fused image, and it also prevents the blocking effects in the output image.

The rest of this paper is arranged as what follows: In the second section, a complete description of the proposed methods is introduced. Then in Section 3, the proposed algorithms are assessed with the previous prominent algorithms with different experiments. Finally, we conclude the paper.

III. PROPOSED METHODS

2.1 DCT

In order to abridge the description of the proposed algorithms, two images were considered for image fusion process, although these algorithms could be used for more than two multi-focus images. We assumed that the input images were aligned by an image registration method. Figures 1 and 2 show two general structures of the proposed methods for fusion of the two multi-focus images. In what follows, we explain the steps of the proposed methods.

As the general structure of the first proposed approach is shown in figure 1, after dividing the source images into 8×8 blocks, their DCT coefficients are calculated. Then the artificial blurred blocks are obtained using the DCT representation of 8×8 blocks by the proposed DCT filtering method. In this paper, a new approach with vector processing is proposed for passing the blocks through a low-pass filter in the DCT domain. Mathematical calculations of the proposed DCT filtering are described in Section

2.3. It is obvious that the difference between the sharp image and its corresponding blurred image is more than the difference between the unsharped image and its corresponding blurred image. Therefore, the block that comes from a part of the focused image and has more details is changed more when it is passed through a low-pass filter. Consequently, the correlation coefficient value between the blocks before and after passing through a low-pass filter has a lower value for the focused block than the non-focused block.

Therefore, those blocks that are changed more due to passing through a low-pass filter have lower correlation coefficient values, so they are more suitable for selection in the output fused image. Following the aforementioned reason, condition (1) (given below) is suggested. Suppose that imA and imB belong to the focused and non-focused area, respectively. Condition (2) is redefined from condition (1) using a simple mathematical action.

$$corr(imA,imA) < corr(imB,imB) \qquad (1)$$

$$(1 - corr(imA,imA)) > (1 - corr(imB,imB)) \qquad (2)$$

On the other hand, the block energy is a useful criterion for measurement of the image contrast in that region. The main reason could be more details of the focused image and its larger coefficient value compared with the part of the non-focused image. This criterion has a significant impact on our algorithm in two stages. In the first stage, the energy of input images for each divided block is calculated. The block that has the highest energy should be selected for the output image. This selection is done using condition (3). In the second stage, the energy criterion can be used for the artificial blurred blocks that are obtained from the input blocks using condition (4).

$$energy(imA) > energy(imB) \qquad (3)$$

$$energy(imA) > energy(imB) \qquad (4)$$

where, imA, imB, and   are the first input image block, artificial blurred of first input image block, second input image block, and artificial blurred of second input image block, respectively. A better output image quality is achieved using the correlation coefficient criterion for both energy measurements of block given in (3) and (4). The final condition is expressed as (5) by combining conditions (2), (3), and (4).

$$energy(imA) \times (1 - corr(imA,imA)) \times$$
$$energy(\overline{imA}) \ > \ energy(imB) \times \qquad (5)$$
$$(1 - corr(imB,\overline{imB})) \times energy(imB)$$

Condition (6), a simple form of condition (5), is the condition of the proposed method displayed by the Eng_Corr symbol.

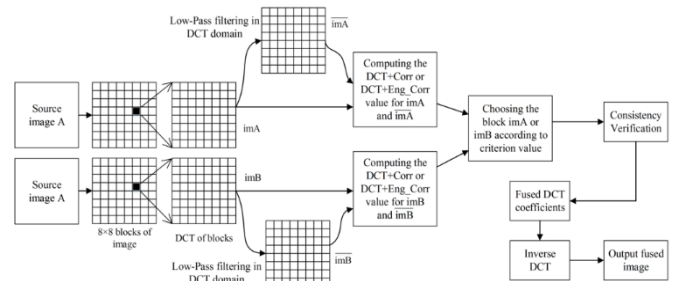$$Eng\_Corr(imA,\overline{imA})) > Eng\_Corr(imB,\overline{imB})) \qquad (6)$$

Figure 1. General structure of first approach in proposed methods
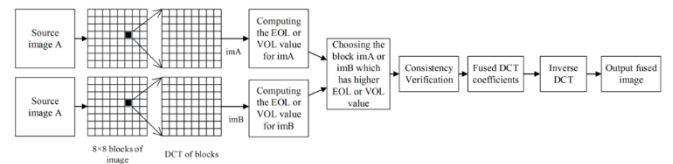

Figure 2. General structure of second approach in proposed methods.

In the second approach of the proposed methods, the focused block with two powerful focus measurements as EOL and VOL is selected. The region of the focused image has more information and high contrast. Subsequently, this region has more raised and evident edges. The amount and intensity of edges in an image are used as a criterion to specify the image quality and contrast. EOL and VOL are two appropriate measurements showing the amount of edges in an image. Therefore, the image block that comes from the focused area has higher EOL and VOL values than the block of the non-focused area. Thus the EOL and VOL values are calculated for every 8×8 block (imA and imB) in the DCT domain. The block with higher EOL or VOL values is considered as the focused area, and is selected for the output image.

Convolving a 3×3 mask on a 8×8 block in DCT domain In order to convolve the 3×3 mask on an 8×8 block directly in the DCT domain, we have proposed a new method by defining 8×8 matrices multiplied on the given block [32]. If the size of the mask is increased, the quality of the fused image by the proposed

algorithms will be reduced for all kinds of multi-focus images in our implemented experiments. Besides this, with increase in the size of the mask, the algorithm complexity and computation time increase. In addition, for 8×8 blocks, 3×3 is very suitable. 5×5 is very large for an 8×8 block. The size of the mask is usually odd due to symmetry, which is logic in image processing. Therefore, according to the numerous conducted experiments, the 3×3 size of the mask is the best one for filtering the 8×8 blocks in terms of the output fused image quality, and also less algorithm complexity.

A 2D DCT of an N×N block of image b is given as (7):

$$B = C.b.C^{\,t} \tag{7}$$

decomposition are considered and simulated using "Image Fusion Toolbox", provided by Oliver Rockinger. However, an online database was used for simulation of the DCHWT method. The DCT+Average, DCT+Contrast, DCT+ AC_Max, and DCT+SF methods were simulated using MATLAB with the best performance conditions.

To evaluate the proposed methods and compare their results with the results of the previous outstanding mentioned methods, the experiments were conducted on two types of test images. The first type of test images is referenced images, and their ground-truth images are available. Typical gray-scale 512×512 test images, given in figure 4, are the referenced-images, which are obtained from an online database. The 16 pair multi-focus test images were generated from eight standard test images given in figure 4. For each pair, the non-focused conditions were created by artificial blurring of images using two disk averaging filters of radii 5 and 9 pixels, separately. These images are blurred in both right and left halves of the images. The second type of test images is non-referenced images, and their ground-truth images are not available. The real multi-focus images were captured with different depths of focus in camera. Two well-known non- referenced images "Disk" 580×640 from an online database and "Book" 960×1280 from an online database were selected.

Figure 4. Standard gray level test images used for simulations

2.3. Performance measurement:

In order to assess the proposed algorithms and compare the given results with those of the previous algorithms, some different evaluation performance metrics of image fusion were used. The mean-squared error (MSE), peak signal-to-noise ratio (PSNR), and structural similarity (SSIM) need the ground-truth image for the referenced images. MSE calculates the total squared error between the ground-truth image and the output fused image, as below:

$$MSE = \frac{1}{mn} \sum_{k=1}^{m} \sum_{l=1}^{n} [G(k,l) - O(k,l)]^2 \tag{44}$$

where, $G(k,l)$ and $O(k,l)$ are the intensity values of the ground-truth image and the output fused image, respectively. The values for m and n are the size of the images.

MSE in the signal/image processing can be converted to PSNR as (45) but it does not have any additional information compared with MSE. Anyway, PSNR calculates the maximum available power of the signal/image over noise, as:

$$PSNR = 10 \log_{10}\left(\frac{L^2}{MSE}\right) \tag{45}$$

where, L is an admissible dynamic range of image pixel values, and is equal to 2b–1 (b=8 bits).

Structure similarity (SSIM) index is a criterion to measure the structure similarity between images x and y as:

$$SSIM(x, y) = \frac{(2\mu_x\mu_y + \mu_1)(2\sigma_{xy} + c_2)}{(\mu_x^2 + \mu_y^2 + c_1)(\sigma_x^2 + \sigma_y^2 + c_2)} \quad (46)$$

where, μ_x and μ_y are the mean values of images x and y, respectively; σ_x and σ_y are the variance of images x and y, respectively; and σ_{xy} is the covariance of images x and y. The c_1 and c_2 for 8 bit images are defined as $c_1=(k_1L)^2$ and $c_2=(k_2L)^2$, respectively, where $k_1=0.01$, $k_2=0.03$, and $L=255$.

$Q^{AB/F}$, $L^{AB/F}$, and $N^{AB/F}$ are used for the non- referenced images provided by Xydeas and Petrovics. Consider F as the fused imageof the two input images A and B. The Sobel edge operator is applied for each pixel to get the edge strength and orientation as below (e.g. for input image A):

$$g_A(n,m) = \sqrt{s_A^x(n,m)^2 + s_A^y(n,m)^2} \quad (47)$$

$$\alpha_A(n,m) = \tan^{-1}\left(\frac{s_A^y(n,m)}{s_A^x(n,m)}\right) \quad (48)$$

IV. FUSION RESULT EVALUATION

Secondly, the proposed methods and the other ones are evaluated by real multi-focus images with different depths of focus in camera. The methods were applied on the various sizes of images like "Disk" 580×640 and "Book" 960×1280, so evaluation results for the performance metrics (QAB/F, LAB/F, NAB/F, and FMI) were obtained and listed in table 2. The non- reference multi-focus image fusion metrics values for the realistic images emphasize the advantages of the proposed methods over the other ones. The output fused images of the proposed methods and the „„Book‟‟ source images focusing on the left and the right are shown in figure 5. Beside this, the magnified output images of the proposed and previous methods are shown in figure 5. There are some undesirable side-effects like blurring in the DCT+Average and DCT+Contrast methods. However, the ringing artefacts in wavelet-based methods, and blocking effects/unsuitable block selection in the DCT+Variance, DCT+AC_Max, and

DCT+SF methods could be concluded from the output image results. All the proposed methods could enhance the quality of output fused image and reduce unsuitable block selection significantly. Similarly, the „„Disk‟‟ source multi- focus images and the results of the proposed methods (DCT+Eng_Corr and DCT+Eng_Corr+RCV) are shown in figure 6.

However, the RCV process and the CV process, as the post-processing, are applied on the DCT- based methods for fusion of "Book" images and 16 pair multi-focus images that were generated. The evaluation performance metrics of CV and RCV are listed in table 3. The results obtained showed that although CV enhanced the quality of the output fused image in most cases, the ability of RCV was more than CV in enhancing the quality of output fused image. In addition, RCV could prevent the unsuitable block selection significantly and remove the blocking effects completely in the output fused image. The visual comparison of CV and RCV of the "Book" image, shown in figure 7 demonstrate this claim.

In another experiment, the proposed methods and the pervious ones were conducted on the "Lena" and "Pepper" multi-focus images. The non- focused conditions of these multi-focus images were created by artificial blurring of images using a disk averaging filter of radius 9 pixel. The PSNR values for the fused output image of different methods are recorded in table 4. It is understandable that the PSNR values for the results of the latest method for "Lena" is infinite (∞). Focused block recognition of "Lena" is easy because of the inherent high local correlation among pixel values and high contrast between adjacent areas, whereas the focused block recognition of "Pepper" is harder than "Lena". Thus we conducted experiments on "Pepper" as a harder quality test in order to compare the methods in fair conditions. All proposed methods have better results over the previous ones. The ground-truth image, multi-focus images of "Pepper", difference images between the ground- truth images, fused output images of the proposed methods, and other methods are

depicted in figure 7. DCT+VOL+RCV and DCT+Eng_Corr+RCV have the best results in the PSNR values, and have less image differences in table 4 and figure 7, respectively.

In this paper, four new multi-focus image fusion methods are introduced. All the proposed methods have significant improvements in the quality of the output fused images. In fact, all the DCT- based fusion methods for JPEG image are less time-consuming and suitable for implementation in real-time applications. However, it is important that which one is faster in order to implement in the real-time applications. We conducted an average run-time comparison for our proposed methods in table 5. Our proposed algorithms were performed using the MATLAB 2016b software with an 8 GB RAM and Intel core i7-7500 CPU processor @ 2.7GHz & 2.9 GHz. According to table 5, DCT+Vol has the best run-time (0.110408 s) for fusion of 512×512 multi-focus images, and next, DCT+Eol, DCT+Corr, and DCT+Eng+Corr have 0.124598, 0.160410, and 0.173938 srun times, respectively. DCT+VOL has a better image quality and faster algorithm run-time than DCT+Corr & DCT+EOL. According to tables 1, 2, 3, and 4, the best quality result is for DCT+Eng_Corr, and after that is for DCT+VOL. Thus we can conclude that DCT+Eng_Corr is a better choice if the powerful hardware is available, and time-consumption has little importance. On the other side, DCT+VOL is a better choice if there is a critical need for time and energy-consumption. Anyway, all proposed methods have significant improvement in quality of the output fused images, and are appropriate for real-time applications due to implantation in the DCT domain.

V. CONCLUSION

In this paper, four new multi-focus image fusion methods were introduced completely in the DCT domain. By proposing an algorithm for convolving a mask on the 8×8 block directly in the DCT domain, we could calculate the image Laplacian and image low-pass filtering in DCT domain. Thus two powerful Laplacian-based focus measurements, VOL and EOL were implemented in the DCT domain. Two other powerful DCT focus measurements, DCT+Corr and DCT+Eng_Corr, were introduced. These methods measure the occurring changes in passing image blocks through the low-pass filter in the DCT domain. In addition, we substituted CV post- processing with RCV. This replacement improved the quality of the output fused image significantly and prevents unsuitable block selection and blocking effects in the output fused image. We conducted a lot of experiments on various types of multi-focus images. The accuracy of the proposed methods is assessed by applying the proposed algorithms and other well-known methods on the several referenced images and non-referenced images. However, evaluation of different methods was done using various evaluation performance metrics. The results obtained show the advantages of the proposed algorithms over some precious and the state of art algorithms in terms of quality of output image. In addition, due to a simple implementation of the proposed algorithms in the DCT domain, they are appropriate for use in real- time applications.

Table 1. MSE and SSIM comparison of various image fusion methods on reference images.

| Methods	Average values for 16 pairs images created from image shown in Fig. 4	
	MSE	SSIM
DCT+Average [28]	65.1125	0.9164
DCT+Contrast [28]	23.0788	0.9647
DWT [23]	19.2411	0.9619
SIDWT [24]	15.5693	0.9641
DCHWT [25]	4.7756	0.9902
DCT+Variance [27]	17.2293	0.9720
DCT+AC_Max [29]	4.1520	0.9917
DCT+SF [30]	5.6848	0.9896
DCT+SML [31]	9.8444	0.9828
DCT+ EOL (proposed)	2.5487	0.9944
DCT+VOL (proposed)	2.5486	0.9944
DCT+Corr (proposed)	5.2722	0.9921
DCT+Eng_Corr (proposed)	1.9594	0.9950

Table 2. $Q^{AB/F}$, $L^{AB/F}$, $N^{AB/F}$, and FMI comparison of various image fusion methods on non-referenced images

Methods	"BOOK"				"DISK"			
	$Q^{AB/F}$	$L^{AB/F}$	$N^{AB/F}$	FMI	$Q^{AB/F}$	$L^{AB/F}$	$N^{AB/F}$	FMI
DCT+Average [28]	0.4985	0.5002	0.0025	0.9075	0.5187	0.4782	0.0063	0.9013
DCT+Contrast [28]	0.6470	0.2384	0.3736	0.9074	0.6212	0.2554	0.3629	0.8981
DWT [23]	0.6621	0.2294	0.3569	0.9117	0.6302	0.2552	0.3362	0.9039
SIDWT [24]	0.6932	0.2637	0.1279	0.9122	0.6694	0.2764	0.1564	0.9049
DCHWT [25]	0.6684	0.3014	0.0705	0.9123	0.6529	0.3140	0.0789	0.9075
DCT+Variance [27]	0.7210	0.2660	0.0277	0.9135	0.7165	0.2612	0.0478	0.9070
DCT+AC_Max [29]	0.7081	0.2781	0.0294	0.9136	0.6763	0.2910	0.0696	0.9057
DCT+SF [30]	0.7151	0.2757	0.0197	0.9148	0.7213	0.2600	0.0415	0.9086
DCT+SML [31]	0.6960	0.2928	0.0241	0.9147	0.6774	0.3074	0.0324	0.9080
DCT+ EOL (proposed)	0.7283	0.2620	0.0206	0.9153	0.7280	0.2522	0.0425	0.9094
DCT+VOL (proposed)	0.7284	0.2619	0.0207	0.9153	0.7285	0.2519	0.0421	0.9094
DCT+Corr (proposed)	0.7281	0.2622	0.0207	0.9153	0.7246	0.2541	0.0456	0.9087
DCT+Eng_Corr (proposed)	0.7284	0.2622	0.0202	0.9155	0.7288	0.2530	0.0391	0.9094

Figure 5. Source images "Book" and fusion results. (a) First source image with focus on the right. (b) Second source image with focus on the left. (c) DCT + EOL (proposed) result. (d) DCT+VOL(proposed). (e) DCT+Corr(proposed). (f) DCT+Eng_Corr (proposed). (g), (h), (i), (j), (k), (l), (m), (n), (o), (p), (q), (r), and (s) are the local magnified versions of DCT+Average, DCT+Contrast, DWT, SIDWT, DCHWT, DCT+Variance, DCT+Ac_Max, DCT+SF, DCT+SML, DCT+EOL(proposed), DCT+VOL(proposed), DCT+Corr(proposed), and DCT+Eng_Corr (proposed), respectively.

<table>
| (a) | (b) | (c) | (d) |
</table>
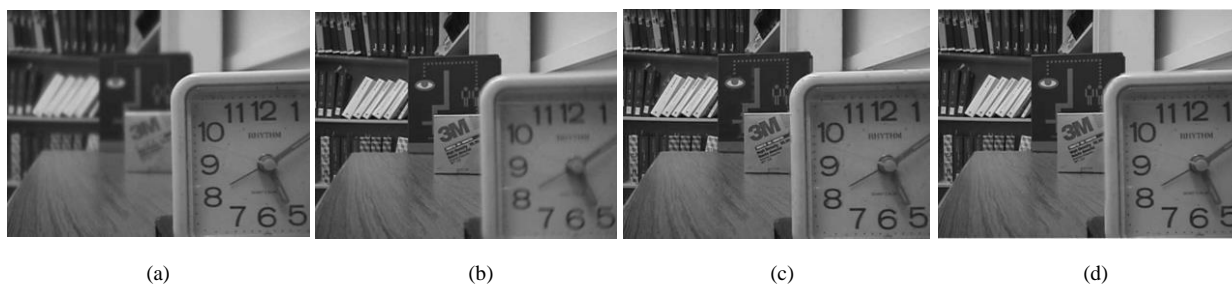
Figure 6. Source images "Disk" and fusion results. (a) First source image with focus on the right. (b) Second source image with focus on the left. (c) DCT+Eng_Corr (proposed). (d) DCT+Eng_Corr+RCV (proposed)

Table 4. PSNR comparison between multi-focus image fusion methods on "Lena" and "House" images

Methods	PSNR (dB)	
	"Lena"	"Pepper"
DCT+Average [28]	29.6283	29.6283
DCT+Contrast [28]	32.3775	33.3672
DWT [23]	34.8943	33.7156
SIDWT [24]	36.0411	34.6095
DCHWT [25]	40.8483	42.9835
DCT+Variance+CV [27]	34.3470	33.5931
DCT+AC_Max+CV [29]	∞	40.8329
DCT+SF+CV [30]	39.5646	40.4470
DCT+SML+CV [31]	∞	35.1566
DCT+ EOL+CV (proposed)	∞	44.0011
DCT+VOL+CV (proposed)	∞	44.0011
DCT+Corr+CV (proposed)	∞	40.3896
DCT+Eng_Corr+CV (proposed)	∞	48.6852
DCT+VOL+RCV (proposed)	∞	48.4816
DCT+Eng_Corr+RCV (proposed)	∞	54.3365

Table 5. Average Run-Time comparison between four proposed 512×512 multi-focus image fusion methods.

Methods	Time (s)
DCT+ EOL (proposed)	0.124598
DCT+VOL (proposed)	0.110408
DCT+Corr (proposed)	0.160410
DCT+Eng_Corr (proposed)	0.173938

VI. REFERENCES

[1]. Drajic, D. & Cvejic, N. (2007). Adaptive fusion of multimodal surveillance image sequences in visual sensor networks. IEEE Transactions on Consumer Electronics, vol. 53, no. 4, pp. 1456-1462.

[2]. Wu, W., Yang, X., Pang, Y., Peng, J. & Jeon, G. (2013). A multifocus image fusion method by using hidden Markov model. Optics Communication, vol. 287, January, pp. 63-72.

[3]. Kumar, B., Swamy, M. & Ahmad, M. O. (2013). Multiresolution DCT decomposition for multifocus image fusion. In 26th Annual IEEE Canadian Conference on Electrical and Computer Engineering (CCECE), pp. 1-4.

[4]. Haghighat, M. B. A, Aghagolzadeh, A. & Seyedarabi, H. (2010). Real-time fusion of multi-focus images for visual sensor networks. In 6th Iranian Machine Vision and Image Processing (MVIP), pp. 1- 6.

[5]. Naji, M. A., & Aghagolzadeh, A. (2015). A new multi-focus image fusion technique based on variance in DCT domain. In 2nd International Conference on Knowledge-Based Engineering and Innovation (KBEI), pp. 478-484.

[6]. Castanedo, F., García, J., Patricio, M., & Molina, J.M. (2008). Analysis of distributed fusion alternatives in coordinated vision agents. In 11th International Conference on Information Fusion, pp. 1-6.

[7]. Kazemi, V., Seyedarabi, H. & Aghagolzadeh, A. (2014). Multifocus image fusion based on compressive sensing for visual sensor networks. In 22nd Iranian Conference on Electrical Engineering (ICEE), pp. 1668-1672.

[8]. Soro, S., & Heinzelman, W. (2009). A Survey of Visual Sensor Networks. Advances in Multimedia. vol. 2009, Article ID 640386, 21 pages, May.

[9]. Huang, W. & Jing, Z. (2007). Evaluation of focus measures in multi-focus image fusion. Pattern Recognition Letters, vol. 28, no. 4, pp. 493-500.

[10]. Li, S., Kwok, J. T., & Wang, Y. (2001). Combination of images with diverse focuses using the spatial frequency, Information fusion, vol. 2, no. 3, pp. 169-176.

[11]. Li, S., & Yang, B. (2008). Multifocus Image Fusion Using Region Segmentation and Spatial Frequency. Image and Vision Computing, vol. 26, no. 7, pp. 971-979.

[12]. Hongmei, W., Cong, N., Yanjun, L., & Lihua, C. (2011). A Novel Fusion Algorithm for Multi-focus Image. International Conference on Applied Informatics and Communication (ICAIC), pp. 641-647.

[13]. Mahajan, S., & Singh, A. (2014). A Comparative Analysis of Different Image Fusion Techniques. IPASJ International Journal of Computer Science (IIJCS), vol. 2, no. 1, pp. 634-642.

[14]. Pertuz, S., Puig, S. D., & Garcia, M. A. (2013). Analysis of focus measure operators for shape-from- focus. Pattern Recognition. Vol. 46, no. 5, pp.1415- 1432.

[15]. Kaur, P., & Kaur, M. (2015). A Comparative Study of Various Digital Image Fusion Techniques: A Review. International Journal of Computer Applications, vol. 114, no. 4.

Cite this Article